

Power Beacon Energy Consumption Minimization in Wireless Powered Backscatter Communication Networks

Haohang Yang, Yinghui Ye, Kai Liang, Xiaoli Chu, *Senior Member, IEEE*

Abstract—Internet-of-Things (IoT) networks are expected to support the wireless connection of massive energy limited IoT nodes. The emerging wireless powered backscatter communications (WPBC) enable IoT nodes to harvest energy from the incident radio frequency signals transmitted by a power beacon (PB) to support their circuit operation, but the energy consumption of the PB (a potentially high cost borne by the network operator) has not been sufficiently studied for WPBC. In this paper, we aim to minimize the energy consumption of the PB while satisfying the throughput requirement per IoT node by jointly optimizing the time division multiple access (TDMA) time slot duration and backscatter reflection coefficient of each IoT node and the PB transmit power per time slot. As the formulated joint optimization problem is non-convex, we transform it into a convex problem by using auxiliary variables, then employ the Lagrange dual method to obtain the optimal solutions. To reduce the implementation complexity required for adjusting the PB's transmit power every time slot, we keep the PB transmit power constant in each time block and solve the corresponding PB energy consumption minimization problem by using auxiliary variables, the block coordinated decent method and the successive convex approximation technique. Based on the above solutions, two iterative algorithms are proposed for the dynamic PB transmit power scheme and the static PB transmit power scheme. The simulation results show that the dynamic PB transmit power scheme and the static PB transmit power scheme both achieve a lower PB energy consumption than the benchmark schemes, and the former achieves the lowest PB energy consumption.

Index Terms—Backscatter communication, energy consumption, IoT, power beacon, resource allocation.

I. INTRODUCTION

WITH the fast development and wide adoption of the Internet-of-Things (IoT) systems, a great number of low-power IoT nodes are being deployed to collect data and deliver them to the information fusion (IF), e.g., a gateway, for information processing [1]. However, due to the cost and form factor constraints, mobile IoT devices are typically powered by batteries with a limited capacity, which can be quickly drained by power-hungry radio frequency (RF) components, e.g., oscillators [2]. To overcome the battery imposed limit, wireless powered backscatter communications (WPBC) [1],

[3] have been proposed to allow an IoT node to modulate and backscatter the incident RF signals transmitted by a power beacon (PB) to carry the IoT node's information to the destination node, while harvesting energy from the PB's RF signals to support the circuit operation.

Various resource allocation schemes for WPBC have been developed to optimize different performance metrics, e.g., sum throughput, user-centric and system-centric energy efficiency (EE) ¹ under the energy-causality constraint per IoT node. However, there is no study working on the energy efficient resource allocation scheme for WPBC from the network operator's perspective, e.g., minimizing the energy consumption of the PB. Such a scheme is vital for the deployment of WPBC in IoT networks, this is because the energy consumption of the user side is usually low and can be satisfied by the harvested energy in WPBC, but the energy consumption of the PB has significant impacts on the cost of the network operator. Motivated by this observation, in this paper, we design an energy efficient resource allocation scheme that minimizes the energy consumption of the PB while satisfying the throughput requirement per IoT node in a WPBC network with multiple IoT nodes.

A. Related Works and Motivations

Some related works on BackCom are listed as follows. In [4], using tools from the stochastic geometry and modeling the IoT nodes and the PB as the random Poisson cluster process, respectively, the authors derived the successful transmission probability of a large-scale WPBC network. It revealed that the average network capacity (or the successful transmission rate of a backscatter link) first increases and then decreases with the increasing duty cycle (or the backscatter reflection coefficient). The authors of [5] maximized the throughput of an IoT node for single-user, single-carrier WPBC by jointly optimizing the backscatter reflection coefficient and the time for energy harvesting and that for backscatter communication (BackCom). Subsequently, this work was extended to a single-user, multi-carrier WPBC network, where the total throughput was maximized by jointly optimizing the transmit power on each subcarrier, the backscatter reflection coefficient, the energy harvesting (EH) time and the BackCom time [6].

¹User-centric EE refers to the ratio of the throughput to the energy consumption cost by a user, while the system-centric EE is the EE of the whole network, which includes all the users, PBs and other communication equipments.

Haohang Yang and Xiaoli Chu are with the Department of Electronic and Electrical Engineering, University of Sheffield, Sheffield, S1 4ET, United Kingdom (e-mail: hyang42@sheffield.ac.uk, x.chu@sheffield.ac.uk).

Yinghui Ye is with the Shaanxi Key Laboratory of Information Communication Network and Security, Xi'an University of Posts & Telecommunications, China (e-mail: connectyuh@126.com).

Kai Liang is with the State Key Laboratory of Integrated Service Networks, Xidian University, Xi'an 710071, China (e-mail: kliang@xidian.edu.cn).

The PB's signal waveform design and the associated tradeoff between the harvested energy of the IoT node and the signal-to-interference-plus-noise ratio (SINR) of the IoT node to the associated receiver link were studied for a single-user WPBC network in [7] and for a multi-user WPBC network in [8]. In [9], the rate-energy tradeoff was studied for both power splitting and time switching-based WPBC networks. The authors of [10], [11] developed resource allocation schemes to maximize the system-centric energy efficiency, which was defined as the ratio of the total throughput of the network to the total energy consumption of a network, in a WPBC system with or without quality of service (QoS) constraints of IoT nodes, respectively. In [12], the authors jointly optimized the backscatter reflection coefficient of each IoT node and the transmit power of a PB to maximize the minimum energy efficiency of all the IoT nodes, subject to the QoS requirement per IoT node.

The combination of WPBC and active transmissions (AT), where the IoT nodes convey information via hybrid BackCom and AT using the harvested energy, has also been studied. In [13], the Stackelberg game was employed to jointly maximize the PB's revenue and the IoT nodes' utility function. In [14], the time allocated for EH, BackCom, and AT was optimized to maximize the total throughput of a multi-user hybrid BackCom-AT network. The sum throughput of all IoT nodes was maximized by optimizing the time allocation for EH, BackCom and AT in hybrid WPBC-AT-based heterogeneous networks [15] and hybrid WPBC-AT-based cognitive radio networks [16], respectively. To ensure the throughput fairness among IoT nodes in a hybrid BackCom-AT network, the authors in [17] solved a max-min throughput problem by jointly optimizing the backscatter reflection coefficient, the time for EH, BackCom and AT, and the transmit power of AT for each IoT node. Hybrid WPBC-AT was also employed in relay networks to enhance the achievable throughput of the IoT nodes by jointly optimizing the AT time and transmit power of the relay node [18] or by optimizing the backscatter reflection coefficient of the relay node [19]. The authors of [20] maximized the user-centric energy efficiency, which was defined as the ratio of the throughput of an IoT node to the energy consumption of the IoT node, in a single-user hybrid WPBC-AT-enabled cognitive radio network [20]. In [21], the total user-centric energy efficiency of all IoT nodes was maximized by jointly optimizing the transmit power of the PB and each IoT node's time for BackCom and AT under a non-linear energy harvesting model.

We note that the existing works on energy efficient or spectral efficient resource allocation schemes for WPBC are mainly from the system perspective with the assumption of signal user [10], [11] or the user perspective [20], [21]. Also, the energy consumption of the operator, e.g., a PB, is much higher than that of the users in WPBC networks due to their passive backscatter circuit. Thus, the energy consumption minimization scheme from the network operator's perspective with multiple users has not been studied and this motivates this work.

B. Contributions

In this paper, we consider a WPBC network of multiple IoT nodes, where in each time block, the IoT nodes take turns to modulate their own information on the incident RF signal from the PB and backscatter it to the IF following a time-division multiple-access (TDMA) protocol, and devise resource allocation schemes to minimize the energy consumption of the PB while satisfying the throughput requirement of each IoT node. Our main contributions are summarized as follows.

- The energy consumption of the PB in each time block is minimized by jointly optimizing the PB transmit power per time slot, the TDMA time slot duration and backscatter reflection coefficient of each IoT node, while guaranteeing the throughput requirements of the IoT nodes. By solving this joint optimization problem, we propose a dynamic PB transmit power scheme, where the PB adjusts its transmission power in each TDMA time slot according to the channel condition from the corresponding IoT node to the IF and to itself to minimize the PB's energy consumption in a time block. Considering the implementation complexity required for adjusting the PB's transmit power every time slot, we also propose a reduced-hardware complexity static PB transmit power scheme, where the PB transmit power remains constant in a transmission block and is optimized to minimize the PB energy consumption in each time block.
- Due to multiple coupled variables in the objective function and the constraints, the two formulated optimization problems are non-convex and hard to solve directly. In the dynamic PB transmit power scheme, we use two auxiliary variables to transform the original optimization problem into a convex form and prove the convexity. Although the problem is transformed to be convex, we cannot simply use CVX tool to solve it due to the fractional form in some constraints. Instead, we employ the Lagrange dual method to solve it and derive the closed-form expressions of the optimal PB transmit power per time slot and the optimal backscatter reflection coefficients of the IoT nodes. In the static PB transmit power scheme, since the non-convex optimization problem cannot be transformed into a convex form, we employ the successive convex approximation (SCA) technique and block coordinated decent (BCD) method to solve the problem and obtain sub-optimal solutions of the PB transmit power and the IoT nodes' time slot durations and backscatter reflection coefficients. Based on the above solutions, we propose two iterative algorithms for the dynamic PB transmit power scheme and the static PB transmit power scheme, respectively.
- We obtain and theoretically prove the following key insight. In the dynamic PB transmit power scheme, the PB energy consumption is minimized when the entire time block is used up for EH and BackCom by all the IoT nodes, but it may not be the case for the static PB transmit power scheme. The convergence and the run time of the proposed algorithms are analysed. Simulation results are presented to evaluate the convergence and the PB energy

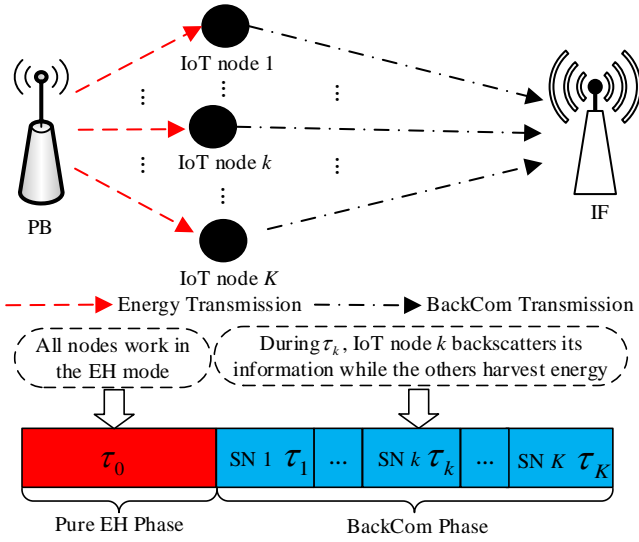


Fig. 1: System model and time structure.

consumption performance of the proposed algorithms in comparison with the benchmark schemes that maximize the EE or the throughput.

The rest of the paper is organized as follows. The system model is presented in Section II. In Section III and Section IV, the PB energy consumption minimization problems for the two schemes are formulated and solved, respectively. Section V analyses the convergence and the run time of the proposed algorithms. In Section VI, the numerical results are presented. Section VII concludes the paper.

II. SYSTEM MODEL

As shown in Fig. 1, we consider a WPBC network, which consists of one PB, K IoT nodes and one IF. Both the PB and IF have stable power supply, while the K IoT nodes are equipped with backscatter circuits and they are battery powered and energy-constrained. To minimize the battery power consumption at the IoT nodes, each IoT node harvests energy from the incident signal transmitted by the PB to support its own circuit operation and conveys IoT nodes' information to the IF via BackCom following a TDMA protocol. We assume that all devices are equipped with a single antenna. We consider a block flat-fading channel model, where all the channel gains keep constant in one transmission block, but may change across adjacent transmission blocks. Each transmission block has a duration of T seconds, which is shorter than the channel coherence time. As channel estimation is outside the scope of this paper, we assume that the perfect channel state information (CSI) of links from the IoT nodes to the PB and the IF can be obtained by the PB via an advanced channel estimation scheme at the beginning of each transmission block [22]–[24].

There are two phases within each transmission block²,

²Although BackCom allows the IoT nodes realizing the information transmission and EH simultaneously, the harvested energy may not enough support the circuit operation due to the low EH efficiency. Thus, we schedule one phase for pure EH.

i.e., the energy harvesting phase (with a duration of τ_0) and the BackCom phase. In order to reduce the co-channel interference and the complexity of the IF, the BackCom phase is further divided into K slots $\{\tau_k, k = 1, 2, \dots, K\}$ and τ_k is allocated to the k -th IoT node for performing BackCom.

In the EH phase τ_0 , the PB broadcasts energy signals, and the received signal at the k -th IoT node is expressed as

$$y_k = \sqrt{P_0 h_k} x_s + w_{k,p} \approx \sqrt{P_0 h_k} x_s, \quad (1)$$

where x_s is the energy signal following a standard circularly symmetric complex Gaussian distribution, i.e., $x_s \sim \mathcal{CN}(0, 1)$, P_0 , h_k , and $w_{k,p}$ are the transmit power of the PB within τ_0 , the channel gain from the PB to the k -th IoT node, and the thermal noise of the k -th IoT node, respectively. In (1), the approximation is obtained due to the fact that the BackCom circuit only consists of passive components and the value of $w_{k,p}$ is negligible.

In τ_0 , all IoT nodes harvest energy from the broadcasted energy signal. For a practical energy harvester, the harvested power is a non-linear function of the input power. Considering a non-linear EH model [25], the harvested energy of the k -th IoT node within τ_0 can be calculated as

$$E_{\tau_0}^k = \left(\frac{a P_0 h_k + d}{P_0 h_k + v} - \frac{d}{v} \right) \tau_0, \quad (2)$$

where a , d and v are the parameters of the non-linear EH model and can be determined by the experimental fitting approach [25], and $P_0 h_k$ is the input power.

In the BackCom phase, the PB continues to broadcast energy signals and each IoT node takes turns (i.e., in their allocated time slot) to work in the BackCom mode, while all the other IoT nodes continue to harvest energy. In time slot τ_k , the harvested energy of the i -th IoT node, $i = \{1, 2, \dots, K, i \neq k\}$, is expressed as

$$E_{\tau_k}^i = \left(\frac{a P_k h_i + d}{P_k h_i + v} - \frac{d}{v} \right) \tau_k, \quad (3)$$

where P_k is the transmit power of the PB within τ_k .

At the k -th IoT node in time slot τ_k , the incident signal from the PB is split into two parts via a power reflection coefficient β_k , i.e., the part $\sqrt{\beta_k} P_0 h_k x_s$ for carrying the k -th IoT node's information to the IF, and the remaining part $\sqrt{(1 - \beta_k)} P_0 h_k x_s$ flowing into the EH circuit, where $0 \leq \beta_k \leq 1, \forall k$. Then the achievable throughput of the backscatter link from the k -th IoT node to the IF and the harvested energy by the k -th IoT node within τ_k can be written as, respectively,

$$R_k^{\tau_k} = W \tau_k \log_2 \left(1 + \frac{\xi \beta_k P_k h_k g_k}{W N_0} \right), \quad (4)$$

$$E_{\tau_k}^k = \left(\frac{a(1 - \beta_k) P_k h_k + d}{(1 - \beta_k) P_k h_k + v} - \frac{d}{v} \right) \tau_k, \quad (5)$$

where g_k is the channel gain between the k -th IoT node and the IF, W is the channel bandwidth, N_0 is the noise power spectrum density, and $0 < \xi < 1$ is a parameter to describe the performance gap between the BackCom and the

Shannon capacity³. Please note that the IF receives the signals from the k -th IoT node and the PB simultaneously, but the received signal from the PB can be perfectly removed by using successive interference cancellation (SIC). This is because the PB does not transmit information and the energy signal x_s can be predefined and known by the IF. In this case, once the channel coefficient between the PB and the IF is estimated, SIC can be performed.

Based on (2), (3) and (5), the total harvested energy of the k -th IoT node during one transmission block is given by

$$E_k^{\text{total}} = \left(\frac{a(1-\beta_k)P_k h_k + d}{(1-\beta_k)P_k h_k + v} - \frac{d}{v} \right) \tau_k + \sum_{i=0, i \neq k}^K \left(\frac{aP_i h_k + d}{P_i h_k + v} - \frac{d}{v} \right) \tau_i. \quad (6)$$

III. PB ENERGY CONSUMPTION MINIMIZATION WITH DYNAMIC TRANSMIT POWER

In this section, we introduce a dynamic PB transmit power scheme, where the PB's transmit power can be adjusted in every time slot, and formulate a joint optimization problem to minimize the energy consumed by the PB while meeting the throughput requirement of each IoT node, and transform it into a convex problem and solve it by a Lagrange dual method.

A. Problem Formulation

We propose to minimize the energy consumption of the PB by jointly optimizing the time slot durations for EH and BackCom, and the reflection coefficient of each IoT node, and the transmit power of the PB at each time slot, subject to the minimum throughput requirement per IoT node. Mathematically, the problem can be written as

$$\mathcal{P}_1 : \min_{\tau_0, \tau, \beta, P_0, \mathbf{P}} \sum_{i=0}^K P_i \tau_i \quad (7a)$$

$$\text{s.t. C1} : W \tau_k \log_2 \left(1 + \frac{\xi \beta_k P_k h_k g_k}{W N_0} \right) \geq R_k^{\min}, \forall k, \quad (7b)$$

$$\text{C2} : \left(\frac{a(1-\beta_k)P_k h_k + d}{(1-\beta_k)P_k h_k + v} - \frac{d}{v} \right) \tau_k + \sum_{i=0, i \neq k}^K \left(\frac{aP_i h_k + d}{P_i h_k + v} - \frac{d}{v} \right) \tau_i \geq p_{c,k} \tau_k, \forall k, \quad (7c)$$

$$\text{C3} : \tau_0, \tau_k \geq 0, \forall k, \sum_{k=0}^K \tau_k \leq T, \quad (7d)$$

$$\text{C4} : 0 \leq \beta_k \leq 1, \quad (7e)$$

$$\text{C5} : 0 < P_0, P_k \leq P_{\max}, \forall k, \quad (7f)$$

³Due to the passive modulation, the throughput of BackCom is much less than the Shannon capacity. We note that in some works, the achievable rate of BackCom is approximated as a constant that is determined by the experimental testing. Such an approach is valid when the transmit power of a PB and the reflection coefficient keep unchange. In this work, since we jointly optimize the transmit power of the PB and the reflection coefficient of per IoT node, we use the Shannon capacity to approximate BackCom capacity and a parameter is adopted to reflect their performance gap [17].

where $\boldsymbol{\tau} = [\tau_1, \tau_2, \dots, \tau_K]$, $\boldsymbol{\beta} = [\beta_1, \beta_2, \dots, \beta_K]$, $\mathbf{P} = [P_1, P_2, \dots, P_K]$, and R_k^{\min} and $p_{c,k}$ are the minimum required throughput and the circuit power consumption of the k -th IoT node, respectively.

In \mathcal{P}_1 , constraint C1 guarantees that the achievable throughput of the k -th IoT node is above R_k^{\min} . Constraint C2 requires that the consumed energy by the k -th IoT node should not exceed its harvested energy. C3 constrains the EH time and the BackCom time. Constraints C4 and C5 set the value range of the reflection coefficient of the k -th IoT node and the transmit power of the PB, respectively. \mathcal{P}_1 is non-convex due to the coupled variables in the objective function, and constraints C1 and C2. Moreover, C2 contains nonlinear fractional functions due to the use of the non-linear EH model. Therefore, problem \mathcal{P}_1 is non-convex and cannot be directly solved by using existing convex tools, e.g, CVX. In what follows, we will transform \mathcal{P}_1 into a convex problem and propose an iterative algorithm to solve it.

B. Problem Transformation

To decouple the optimization variables P_i and τ_i , we construct a series of auxiliary variables $\theta_i = P_i \tau_i$, $i = 0, 1, \dots, K$, and substitute $P_i = \frac{\theta_i}{\tau_i}$ into \mathcal{P}_0 , which results in

$$\mathcal{P}_{1.1} : \min_{\tau_0, \tau, \beta, \theta_0, \boldsymbol{\theta}} \sum_{i=0}^K \theta_i \quad (8a)$$

$$\text{s.t. C1}' : W \tau_k \log_2 \left(1 + \frac{\xi \beta_k \theta_k h_k g_k}{\tau_k W N_0} \right) \geq R_k^{\min}, \forall k, \quad (8b)$$

$$\text{C2}' : \left(\frac{a(1-\beta_k) \frac{\theta_k}{\tau_k} h_k + d}{(1-\beta_k) \frac{\theta_k}{\tau_k} h_k + v} - \frac{d}{v} \right) \tau_k + \sum_{i=0, i \neq k}^K \left(\frac{a \frac{\theta_i}{\tau_i} h_k + d}{\frac{\theta_i}{\tau_i} h_k + v} - \frac{d}{v} \right) \tau_i \geq p_{c,k} \tau_k, \forall k, \quad (8c)$$

$$\text{C5}' : 0 < \theta_0 \leq P_{\max} \tau_0, 0 < \theta_k \leq P_{\max} \tau_k, \forall k, \quad (8d)$$

C3, C4,

where $\boldsymbol{\theta} = [\theta_1, \theta_2, \dots, \theta_K]$.

In $\mathcal{P}_{1.1}$, the objective function (8a) is linear and thus is more tractable than (7a). However, the reflection coefficient β_k is still coupled with θ_k in C1' and C2'. To address this problem, we further introduce the auxiliary variables $\lambda_k = \beta_k \theta_k$, substitute them into problem $\mathcal{P}_{1.1}$ and have

$$\mathcal{P}_{1.2} : \min_{\tau_0, \tau, \lambda, \theta_0, \boldsymbol{\theta}} \sum_{i=0}^K \theta_i \quad (9a)$$

$$\text{s.t. C1}'' : W \tau_k \log_2 \left(1 + \frac{\xi \lambda_k h_k g_k}{\tau_k W N_0} \right) \geq R_k^{\min}, \forall k, \quad (9b)$$

$$\text{C2}'' : \left(\frac{a(\theta_k - \lambda_k) h_k + d}{\frac{\theta_k - \lambda_k}{\tau_k} h_k + v} - \frac{d}{v} \right) \tau_k + \sum_{i=0, i \neq k}^K \left(\frac{a \frac{\theta_i}{\tau_i} h_k + d}{\frac{\theta_i}{\tau_i} h_k + v} - \frac{d}{v} \right) \tau_i \geq p_{c,k} \tau_k, \forall k, \quad (9c)$$

$$\text{C4}' : 0 \leq \lambda_k \leq \theta_k, \forall k \quad (9d)$$

$$\text{C3, C5}'.$$

$$\begin{aligned} \mathcal{L} = & \sum_{i=0}^K \theta_i + \sum_{k=1}^K \alpha_k \left[p_{c,k} \tau_k - \left(\frac{a(\theta_k - \lambda_k)}{\tau_k} h_k + d - \frac{d}{v} \right) \tau_k - \sum_{i=0, i \neq k}^K \left(\frac{a \theta_i h_k + d}{\tau_i h_k + v} - \frac{d}{v} \right) \tau_i \right] \\ & + \sum_{k=1}^K \varepsilon_k \left[R_k^{\min} - W \tau_k \log_2 \left(1 + \frac{\xi \lambda_k h_k g_k}{\tau_k W N_0} \right) \right] + \vartheta \left[\sum_{i=0}^K \tau_i - T \right] + \sum_{k=1}^K \kappa_k (\lambda_k - \theta_k) + \sum_{i=0}^K \omega_i (\theta_i - P_{\max} \tau_i) \quad (10) \end{aligned}$$

Theorem 1. Problem $\mathcal{P}_{1.2}$ is convex.

Proof. Please refer to Appendix A.

Although problem $\mathcal{P}_{1.2}$ is convex, existing numerical convex program solvers, e.g, CVX tool, cannot directly handle constraint C2'' in (9c) because the CVX tool treats C2'' as a non-convex constraint. Although the successive convex approximation method can be applied on C2'' so that CVX can be employed, such an approach may not be able to provide useful insights into the energy minimization based resource allocation scheme. In view of the above, we leverage the KKT conditions to derive closed-form expressions for some of the optimization variables, thus providing a better understanding of the investigated problem, and devise an iterative algorithm to solve problem $\mathcal{P}_{1.2}$.

C. Problem Solution

The partial Lagrangian function for problem $\mathcal{P}_{1.2}$ is written in (10), as shown at the top of the next page, where $\alpha = [\alpha_1, \alpha_2, \dots, \alpha_K] \succeq \mathbf{0}$, $\varepsilon = [\varepsilon_1, \varepsilon_2, \dots, \varepsilon_K] \succeq \mathbf{0}$, $\kappa = [\kappa_1, \kappa_2, \dots, \kappa_K] \succeq \mathbf{0}$, and $\omega = [\omega_0, \omega_1, \dots, \omega_K] \succeq \mathbf{0}$ are Lagrange multiplier vectors corresponding to constraints C2'', C1'', C4, and C5', respectively, and $\vartheta \geq 0$ is the Lagrange multiplier associated with constraint C3.

Taking the partial derivative of \mathcal{L} with respect to each optimization variable, respectively, we can obtain the following results,

$$\frac{\partial \mathcal{L}}{\partial \theta_0} = 1 - \sum_{k=1}^K \frac{\alpha_k (av - d) h_k}{\left(\frac{\theta_0}{\tau_0} h_k + v \right)^2} + \omega_0, \quad (11)$$

$$\frac{\partial \mathcal{L}}{\partial \theta_k} = 1 - \frac{\alpha_k (av - d) h_k}{\left(\frac{\theta_k - \lambda_k}{\tau_k} h_k + v \right)^2} - \kappa_k + \omega_k, \quad \forall k, \quad (12)$$

$$\frac{\partial \mathcal{L}}{\partial \lambda_k} = \kappa_k + \frac{\alpha_k (av - d) h_k}{\left(\frac{\theta_k - \lambda_k}{\tau_k} h_k + v \right)^2} - \frac{\varepsilon_k W \xi h_k g_k}{\left(W N_0 + \xi h_k g_k \frac{\lambda_k}{\tau_k} \right) \ln 2}, \quad (13)$$

$$\begin{aligned} \frac{\partial \mathcal{L}}{\partial \tau_0} = & - \sum_{k=1}^K \alpha_k \left(a - \frac{d}{v} + \frac{(d - av) \left(\frac{2\theta_0}{\tau_0} h_k + v \right)}{\left(\frac{\theta_0}{\tau_0} h_k + v \right)^2} \right) \\ & + \vartheta - \omega_0 P_{\max}, \quad (14) \end{aligned}$$

$$\begin{aligned} \frac{\partial \mathcal{L}}{\partial \tau_k} = & \alpha_k p_{c,k} - \alpha_k \left(a - \frac{d}{v} + \frac{(d - av) \left(\frac{2(\theta_k - \lambda_k)}{\tau_k} h_k + v \right)}{\left(\frac{\theta_k - \lambda_k}{\tau_k} h_k + v \right)^2} \right) \\ & + \vartheta - \omega_k P_{\max} - \varepsilon_k W \log_2 \left(1 + \frac{\xi \lambda_k h_k g_k}{\tau_k W N_0} \right) \\ & + \frac{\varepsilon_k W \xi h_k g_k \frac{\lambda_k}{\tau_k}}{\left(W N_0 + \xi h_k g_k \frac{\lambda_k}{\tau_k} \right) \ln 2}. \quad (15) \end{aligned}$$

By solving $\frac{\partial \mathcal{L}}{\partial \theta_0} = 0$ for θ_0/τ_0 , the optimal PB transmission power in time slot τ_0 is given by

$$P_0^* = \frac{\theta_0}{\tau_0} = \varphi^{-1}(1 + \omega_0), \quad (16)$$

where $\varphi(x) = \sum_{k=1}^K \frac{\alpha_k (av - d) h_k}{(h_k x + v)^2}$ and $\varphi^{-1}(x)$ denotes its inverse function. As we have shown $av - d > 0$ in Appendix A, $\varphi(x)$ decreases with x for $x \geq 0$ and we can find a unique $\frac{\theta_0}{\tau_0} \geq 0$ satisfying (16) via one-dimensional searching methods.

By letting $\frac{\partial \mathcal{L}}{\partial \theta_k} = 0$ and solving it for $(\theta_k - \lambda_k)/\tau_k$, we have

$$\begin{aligned} P_k^* (1 - \beta_k^*) = & \frac{\theta_k - \lambda_k}{\tau_k} \\ = & \left[\frac{1}{h_k} \sqrt{\frac{\alpha_k (av - d) h_k}{1 + \omega_k - \kappa_k} - \frac{v}{h_k}} \right]^+, \quad (17) \end{aligned}$$

where $[x]^+ = \max\{0, x\}$.

Substituting (17) into (13) and solving $\frac{\partial \mathcal{L}}{\partial \lambda_k} = 0$ for λ_k/τ_k , we obtain

$$P_k^* \beta_k^* = \frac{\lambda_k}{\tau_k} = \left[\frac{\varepsilon_k W}{(\kappa_k + (1 + \omega_k - \kappa_k) \ln 2)} - \frac{W N_0}{\xi h_k g_k} \right]^+. \quad (18)$$

One can see from (18) that $P_k^* \beta_k^*$ increases with $h_k g_k$. This indicates that in order to minimize the energy consumed by the PB, the IoT node with high channel gains from the PB and to the IF should backscatter a large portion of the incident signal power to the IF.

Based on (17) and (18), the optimal P_k is calculated as

$$\begin{aligned} P_k^* = & \left[\frac{1}{h_k} \sqrt{\frac{\alpha_k (av - d) h_k}{1 + \omega_k - \kappa_k} - \frac{v}{h_k}} \right]^+ \\ & + \left[\frac{\varepsilon_k W}{(\kappa_k + (1 + \omega_k - \kappa_k) \ln 2)} - \frac{W N_0}{\xi h_k g_k} \right]^+, \quad (19) \end{aligned}$$

and the optimal β_k is given by

$$\beta_k^* = \frac{1}{\left[\frac{\frac{1}{h_k} \sqrt{\frac{\alpha_k (av-d)h_k}{1+\omega_k - \kappa_k} - \frac{v}{h_k}} \right]^+ + 1} + 1. \quad (20)$$

Substituting (16) into (14), we can rewrite $\frac{\partial \mathcal{L}}{\partial \tau_0}$ as

$$\begin{aligned} \frac{\partial \mathcal{L}}{\partial \tau_0} &= \vartheta - \omega_0 P_{\max} - \sum_{k=1}^K \alpha_k \\ &\times \left(a - \frac{d}{v} + \frac{(d-av)(2\varphi^{-1}(1+\omega_0)h_k+v)}{(\varphi^{-1}(1+\omega_0)h_k+v)^2} \right). \end{aligned} \quad (21)$$

One can observe from (21) that the Lagrangian function (10) is a linear function of τ_0 . By substituting (17) and (18) into (15), we find that $\frac{\partial \mathcal{L}}{\partial \tau_k}$ is free of τ_k , thus the Lagrangian function (10) is also a linear function of τ_k . The above observations indicate that the optimal τ_0 and τ_k can be obtained by solving the following linear programming problem, which is obtained by substituting (16)-(19) into $\mathcal{P}_{1.2}$.

$$\mathcal{P}_{1.3} : \min_{\tau_0, \tau} \sum_{i=0}^K P_i^* \tau_i \quad (22a)$$

$$\text{s.t. } C1''' : W \tau_k \log_2 \left(1 + \frac{\xi \beta_k^* h_k g_k}{W N_0} \right) \geq R_k^{\min}, \forall k, \quad (22b)$$

$$\begin{aligned} C2''' : &\left(\frac{a P_k^* (1 - \beta_k^*) h_k + d}{P_k^* (1 - \beta_k^*) h_k + v} - \frac{d}{v} \right) \tau_k \\ &+ \sum_{i=0, i \neq k}^K \left(\frac{a P_i^* h_k + d}{P_i^* h_k + v} - \frac{d}{v} \right) \tau_i \geq p_{c,k} \tau_k, \forall k, \end{aligned} \quad (22c)$$

C3.

Having obtained $\{\tau_0, \tau, \lambda, \theta_0, \theta\}$ for given Lagrange multipliers, the Lagrange multipliers can be updated in an iterative manner by using the gradient method as follows,

$$\begin{aligned} \alpha_k^{(n+1)} &= \alpha_k^{(n)} - \ell_1 \left(p_{c,k} \tau_k - \left(\frac{a(\theta_k - \lambda_k)}{\tau_k} h_k + d - \frac{d}{v} \right) \tau_k \right. \\ &\quad \left. - \sum_{i=0, i \neq k}^K \left(\frac{a \frac{\theta_i}{\tau_i} h_k + d}{\frac{\theta_i}{\tau_i} h_k + v} - \frac{d}{v} \right) \tau_i \right), \forall k, \end{aligned} \quad (23)$$

$$\varepsilon_k^{(n+1)} = \varepsilon_k^{(n)} - \ell_2 \left(R_k^{\min} - W \tau_k \log_2 \left(1 + \frac{\xi \lambda_k h_k g_k}{\tau_k W N_0} \right) \right), \forall k, \quad (24)$$

$$\omega_i^{(n+1)} = \omega_i^{(n)} - \ell_3 (\theta_i - P_{\max} \tau_i), i = \{0, 1, \dots, K\}, \quad (25)$$

$$\vartheta^{(n+1)} = \vartheta^{(n)} - \ell_4 \left(\sum_{i=0}^K \tau_i - T \right), \quad (26)$$

$$\kappa_k^{(n+1)} = \kappa_k^{(n)} - \ell_5 (\lambda_k - \theta_k), \forall k, \quad (27)$$

where $n \geq 0$ is the iteration index, and $\ell_1, \ell_2, \ell_3, \ell_4$, and ℓ_5 are the step sizes. To guarantee the convergence of the gradient method, the values of the step sizes can be set following [26].

The above Lagrange dual method for solving P1 is summarized in Algorithm 1, where ϕ is the number of iteration.

Algorithm 1 The dynamic PB transmit power scheme

Input: K IoT nodes.

Output: $\tau_0^*, \tau_k^*, \beta_k^*, P_0^*, P_k^*$.

Initialize: $\phi = 0$

- 1: Initialize $\alpha(\phi), \varepsilon(\phi), \kappa(\phi), \omega(\phi), \vartheta(\phi)$.
 - 2: **repeat**
 - 3: Obtain P_k^* and β_k^* from (19) and (20), respectively.
 - 4: Obtain τ_0^* and τ_k^* by solving $\mathcal{P}_{1.3}$ with CVX.
 - 5: $\phi = \phi + 1$;
 - 6: Update $\alpha(\phi), \varepsilon(\phi), \kappa(\phi), \omega(\phi), \vartheta(\phi)$ using (23)-(27).
 - 7: **until** The values of Lagrange multipliers converge.
 - 8: **if** $0 < P_0^*, P_k^* \leq P_{max}$ **then**
 - 9: return $\tau_0^*, \tau_k^*, \beta_k^*, P_0^*, P_k^*$;
 - 10: **else**
 - 11: return $\tau_0^* = 0, \tau_k^* = 0, \beta_k^* = 0, P_0^* = 0, P_k^* = 0$;
 - 12: **end if**
-

D. Insights

By applying the KKT approach to $\mathcal{P}_{1.2}$, we obtain the following two key insights into PB energy minimization based resource allocation scheme

Insight 1. The energy consumed by the PB in a time block is minimized when at least one IoT node consumes all the harvested energy while maintaining its minimum throughput at the minimum required level.

Proof. Please refer to Appendix B.

Insight 2. The PB's energy consumption is minimized when the whole time block is used up for EH and BackCom by all the IoT nodes.

Proof. Please refer to Appendix C.

Remark 1. We can explain **Insight 2** as follows. Since the dynamic PB transmit power scheme allows the PB to use the lowest possible transmit power in each time slot according to the channel conditions from the PB to the corresponding IoT node and from the IoT node to the IF, it allows each IoT node to use the longest possible time duration to perform EH and BackCom to meet their throughput requirement. As a result, the whole time block is used up.

IV. PB ENERGY CONSUMPTION MINIMIZATION WITH STATIC TRANSMIT POWER

In this section, to reduce the implementation complexity required for adjusting the PB's transmit power every time slot, we introduce a static PB transmit power scheme, where the PB transmit power is kept constant in each time block. Accordingly, we formulate another joint optimization problem to minimize the PB energy consumption and solve it by employing the BCD method and the SCA technique.

A. Problem Formulation

Under the condition that the PB transmit power is constant in each time block, we minimize the energy consumption of the PB by optimizing the PB transmit power, the time slot duration and the backscatter reflection coefficient of each IoT node, subject to the minimum throughput requirement of each IoT node. The optimization problem is formulated as

$$\mathcal{P}_2 : \min_{\tau_0, \tau, \beta, P} \sum_{i=0}^K P\tau_i \quad (28a)$$

$$\text{s.t. C1} - 1 : W\tau_k \log_2 \left(1 + \frac{\xi \beta_k P h_k g_k}{W N_0} \right) \geq R_k^{\min}, \forall k, \quad (28b)$$

$$\begin{aligned} \text{C2} - 1 : & \left(\frac{a(1-\beta_k)Ph_k+d}{(1-\beta_k)Ph_k+v} - \frac{d}{v} \right) \tau_k \\ & + \sum_{i=0, i \neq k}^K \left(\frac{aPh_k+d}{Ph_k+v} - \frac{d}{v} \right) \tau_i \geq p_{c,k} \tau_k, \forall k, \end{aligned} \quad (28c)$$

C3; C4,

$$\text{C5} - 1 : 0 < P \leq P_{\max}, \quad (28d)$$

where P denotes the PB transmit power in the current time block.

By observing \mathcal{P}_2 , we can see that replacing $P\tau_i$ by an auxiliary variable, e.g., $P\tau_i = \theta_i$, cannot transform \mathcal{P}_2 into a convex form and the reason is as follows. Since the PB transmit power P is fixed across different time slots in a time block, the above auxiliary variable will lead to another constraint, i.e., $\theta_k/\tau_k = P, \forall k$, which is still non-convex and hard to solve. Thus, in the following, we employ the BCD method and SCA technique to solve \mathcal{P}_2 .

B. Problem Transformation and Solution

For a given P , we can solve \mathcal{P}_2 by employing the BCD method to obtain the sub-optimal solution of the time slot duration and the backscatter reflection coefficient of each IoT node. The obtained solutions can then be substituted into \mathcal{P}_2 to find the sub-optimal solution of P . Thus, \mathcal{P}_2 can be solved in an iterative manner. Next, we introduce the BCD method in details.

For a given P , we introduce the auxiliary variables $L_k = \beta_k \tau_k, \forall k$, substitute them into \mathcal{P}_2 and obtain

$$\mathcal{P}_{2.1} : \min_{\tau_0, \tau, \mathbf{L}} \sum_{i=0}^K P\tau_i \quad (29a)$$

$$\text{s.t. C1} - 2 : W\tau_k \log_2 \left(1 + \frac{\xi L_k P h_k g_k}{W \tau_k N_0} \right) \geq R_k^{\min}, \forall k, \quad (29b)$$

$$\text{C2} - 2 : E_k^{\text{total}'} \left(\frac{L_k}{\tau_k} \right) \geq p_{c,k} \tau_k, \forall k, \quad (29c)$$

C3,

$$\text{C4} - 1 : 0 < L_k \leq \tau_k, \forall k, \quad (29d)$$

$$\begin{aligned} \text{where } \mathbf{L} &= [L_1, L_2, \dots, L_K], \quad E_k^{\text{total}'} \left(\frac{L_k}{\tau_k} \right) = \\ & \left(\frac{a(1-\frac{L_k}{\tau_k})Ph_k+d}{(1-\frac{L_k}{\tau_k})Ph_k+v} - \frac{d}{v} \right) \tau_k + \sum_{i=0, i \neq k}^K \left(\frac{aPh_k+d}{Ph_k+v} - \frac{d}{v} \right) \tau_i. \end{aligned}$$

Following similar steps as in Appendix A, we can prove that $\mathcal{P}_{2.1}$ is a convex problem, but we cannot directly use CVX due to constraint C2 - 2 even though it is convex. Thus, we apply the SCA technique to convert C2 - 2 to a linear form based on **Lemma 1**.

Lemma 1: Letting $Y_k^{(j)} = (\frac{L_k}{\tau_k})^j, j \geq 1$, denote the obtained solution of Y_k after the j th iteration, then it satisfies that [27]

$$E_k^{\text{total}'} \left(\frac{L_k}{\tau_k} \right) \geq E_k^{\text{total}'} (Y_k^{(j)}), \forall k, \quad (30)$$

where

$$\begin{aligned} E_k^{\text{total}'} (Y_k^{(j)}) &= \left(\frac{a(1-Y_k^{(j)})Ph_k+d}{(1-Y_k^{(j)})Ph_k+v} - \frac{d}{v} \right) \tau_k \\ & + \frac{Ph_k d - aPh_k v}{(Ph_k - Y_k^{(j)} Ph_k + v)^2} (L_k - Y_k^{(j)} \tau_k) \\ & + \sum_{i=0, i \neq k}^K \left(\frac{aPh_k+d}{Ph_k+v} - \frac{d}{v} \right) \tau_i, \end{aligned} \quad (31)$$

and the equalities in (30) only hold when $\frac{L_k}{\tau_k} = Y_k^{(j)}$.

Proof. Please refer to Appendix D.

By substituting (31) into $\mathcal{P}_{2.1}$, $\mathcal{P}_{2.1}$ is equivalently transformed into

$$\mathcal{P}'_{2.1} : \{\tau_0^*, \boldsymbol{\tau}^*, \mathbf{L}^*\} = \arg \min_{\tau_0, \tau, \mathbf{L}} \sum_{i=0}^K P\tau_i \quad (32a)$$

s.t. C1 - 2;

$$\text{C2} - 3 : E_k^{\text{total}'} (Y_k^{(j)}) \geq p_{c,k} \tau_k, \forall k, \quad (32b)$$

C3; C4 - 1.

Note that $\mathcal{P}'_{2.1}$ can be directly solved by CVX.

Substituting the obtained $\tau_0^*, \boldsymbol{\tau}^*$ and \mathbf{L}^* into \mathcal{P}_2 , we have

$$\mathcal{P}_{2.2} : \min_P \sum_{i=0}^K P\tau_i \quad (33a)$$

s.t. C1 - 1; C2 - 1; C5 - 1.

According to Appendix A, $\mathcal{P}_{2.2}$ is also a convex problem, and we use the same SCA method for solving $\mathcal{P}_{2.1}$ to transform C2 - 1 into a linear form, then $\mathcal{P}_{2.2}$ can be directly solved by CVX. The transformation and solution process is omitted for brevity.

The above BCD method and SCA technique-based procedure for solving \mathcal{P}_2 is summarized in Algorithm 2, where ϵ denotes the number of iteration.

C. Insights

Insight 3. Different from the dynamic PB transmit power scheme, for the static PB transmit power scheme, we find that minimizing the energy consumption of the PB does not require

Algorithm 2 The static PB transmit power scheme

- 1: K IoT nodes.
 - 2: $\tau_0^*, \tau_k^*, \beta_k^*, P^*$.
 - 3: $\epsilon = 0$
 - 4: Initialize $P(\epsilon)$.
 - 5: **repeat**
 - 6: Obtain $\tau_0^*(\epsilon), \tau_k^*(\epsilon), L_k^*(\epsilon)$ by solving $\mathcal{P}_{2.1}$ with SCA method and CVX.
 - 7: Obtain $\beta_k^*(\epsilon) = \frac{L_k^*(\epsilon)}{\tau_k^*(\epsilon)}$.
 - 8: $\epsilon = \epsilon + 1$.
 - 9: Obtain $P(\epsilon)$ by solving $\mathcal{P}_{2.2}$ with SCA method and CVX.
 - 10: **until** $\tau_0^*(\epsilon), \tau_k^*(\epsilon), L_k^*(\epsilon)$ converge.
 - 11: **if** $0 < P(\epsilon) \leq P_{max}$ **then**
 - 12: return $\tau_0^*, \tau_k^*, \beta_k^*, P^* = P(\epsilon)$;
 - 13: **else**
 - 14: return $\tau_0^* = 0, \tau_k^* = 0, \beta_k^* = 0, P^* = 0$;
 - 15: **end if**
-

the whole time block to be used up for EH and BackCom by all the IoT nodes.

Proof. Please refer to Appendix E.

Remark 2. We can explain Insight 3 as follows. Since the PB transmit power keeps constant during the whole time block, the PB energy consumption is minimized by allocating each IoT node with the minimum required time durations for EH and BackCom that meet their throughput requirement. Thus, the whole time block may not be used up.

V. CONVERGENCE AND RUN TIME ANALYSIS

We first analyze the convergence of Algorithms 1 & 2. In Algorithm 1, i.e., the dynamic PB transmit power scheme, where the Lagrange dual method is used to solve $\mathcal{P}_{1.3}$, since it is a convex problem, the Lagrange multipliers $\alpha, \epsilon, \kappa, \omega, \vartheta$ are guaranteed to converge to the optimal solution of $\mathcal{P}_{1.3}$. In Algorithm 2, i.e., the static PB transmit power scheme, after each iteration of the BCD process, the objective function value of \mathcal{P}'_2 is non-increasing with updated variables. Meanwhile, \mathcal{P}_2 is lower bounded by its constraints. Thus, the BCD method is guaranteed to converge to the locally optimal solutions of \mathcal{P}_2 . Since a convex function is globally lower bounded by its first-order Taylor expansion as given in (30), the achieved value of the objective function is non-increasing after each iteration in $\mathcal{P}'_{2.1}$ and $\mathcal{P}'_{2.1}$ is lower bounded by its constraints. Thus, the SCA technique is guaranteed to converge to the locally optimal solutions of $\mathcal{P}'_{2.1}$ [27].

Next, we evaluate the run time of the proposed Algorithms 1 & 2 through simulations, which are performed using MATLAB 2018 and a laptop with the following configurations: Intel(R) Core(TM) i7-9750H CPU @ 2.6GHZ, RAM 16 GB. In Algorithm 1, the number of iterations for updating the Lagrange multipliers, which is denoted by Δ_1 , is around 3-4, and each iteration spends around 1.33s. Accordingly, the run time of Algorithm 1 is around $1.33\Delta_1$ s. In Algorithm 2, we denote the number of iterations of the BCD process by Δ_2 , and the number of iterations of the SCA process for

solving $\mathcal{P}_{2.1}$ and $\mathcal{P}_{2.2}$ as Δ_3 and Δ_4 , respectively. According to the simulations, the run time of Algorithm 2 is around $\Delta_2(1.284\Delta_3 + 1.296\Delta_4)$ s, where Δ_2, Δ_3 and Δ_4 are in the value ranges of 3-4, 2-3 and 2-3, respectively.

VI. NUMERICAL RESULTS ANALYSIS

In this section, we present numerical results to evaluate the performance of the proposed dynamic PB transmit power scheme and static PB transmit power scheme as compared with two benchmark schemes, which are the EE maximization scheme [28] and the throughput maximization scheme [27]. We assume path loss with distance exponent of α as large scale fading and consider Rayleigh fading following $exp(1)$ as small scale fading. The values of the simulation parameters are listed in **Table 1** unless otherwise specified. .

Table 1 Simulation Parameters

Parameter	Value
Number of IoT nodes K	5
Time block T	10s
Non-linear EH model parameters a, d, v	2.463, 1.635, 0.826 [29]
Channel bandwidth W	400kHz [25]
Noise power spectral density N_0	-110 dBm/Hz [29]
Path loss exponent α	3
Maximum PB transmit power P_{max}	23 dBm
Circuit power consumption of each IoT node $P_{c,k}$	200uw
PB-IF distance r	25m
Minimum throughput requirement of each IoT node R^{min}	2400bit/s

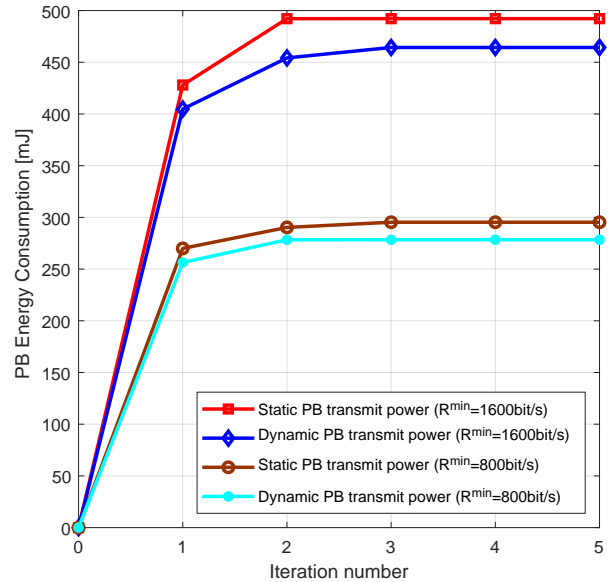


Fig. 2: PB energy consumption versus iteration number ($r = 25m$)

Fig. 2 shows the PB's energy consumption achieved by the proposed Algorithm 1 (the dynamic PB transmit power

scheme) and Algorithm 2 (the static PB transmit power scheme) versus the iteration. We can see that both algorithms converge very fast and that the PB energy consumption of the dynamic PB transmit power scheme is lower than that of the static PB transmit power scheme. This is because in the dynamic scheme, the minimum possible PB transmit power is used in each time slot according to the channel condition from the PB to the corresponding IoT node and from the IoT node to the IF; while in the static scheme, the PB transmit power needs to be high enough to ensure that the IoT node throughput requirement is met even for the IoT node that sees the worst channel condition. Furthermore, the gap between the PB energy consumption achieved by the two schemes increases with the minimum throughput requirement R^{\min} . This indicates that the performance advantage of the dynamic PB transmit power scheme over the static PB transmit power scheme increases with R^{\min} .

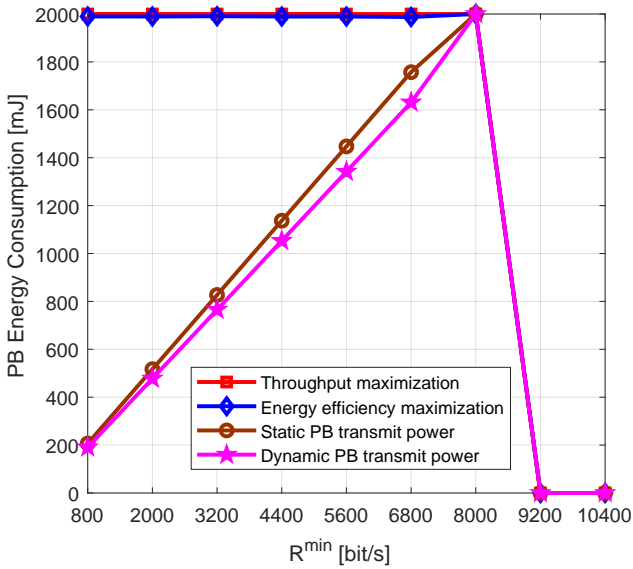


Fig. 3: PB energy consumption versus the minimum required throughput R^{\min} ($r = 25m$)

Fig. 3 plots the PB energy consumption versus the minimum throughput requirement R^{\min} of the IoT nodes under four different schemes. For both the throughput maximization scheme [27] and the EE maximization scheme [28], the maximum possible amount of energy is consumed by the PB in a time block for R^{\min} values up to 8000 bit/s, because both throughput maximization and EE maximization lead to the use of the maximum allowed PB transmit power. For the proposed dynamic PB transmit power scheme and static PB transmit power scheme, the PB energy consumption increases with R^{\min} before it reaches 8000 bit/s, because they both use the minimum possible PB transmit power and transmission time, which increases with the higher throughput requirement. For all the four considered schemes, when R^{\min} exceeds 8000 bit/s, the PB energy consumption drops to 0 since none of them can find a feasible PB transmit power to satisfy the high throughput requirement and the schemes return a zero transmit power of the PB (see Algorithms 1 & 2).

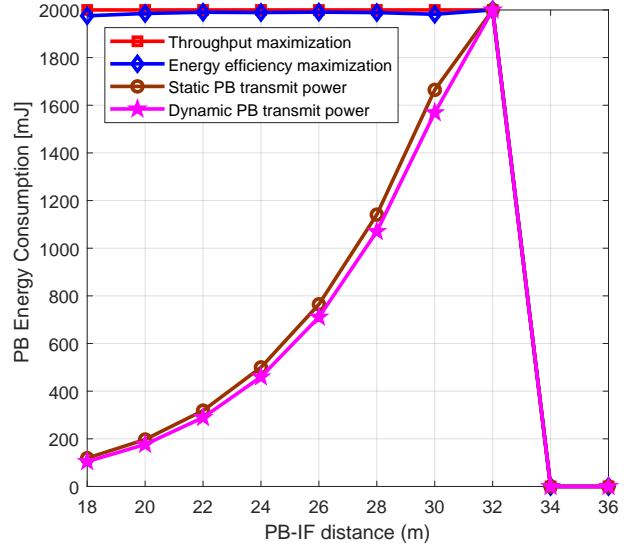


Fig. 4: PB energy consumption versus the PB-IF distance r

Fig. 4 illustrates the PB energy consumption versus the PB-IF distance under the four different schemes. Both the throughput maximization and EE maximization schemes result in the maximum possible PB energy consumption in a time block for PB-IF distances up to 32 m, because they both require the use of the maximum PB transmit power and transmission time. For the proposed dynamic PB transmit power scheme and static PB transmit power scheme, the PB energy consumption increases with a longer PB-IF distance until it reaches 32 m, since the optimized PB transmit power and transmission time increase with the PB-IF distance. When the PB-IF distance goes beyond 32m, the PB energy consumption drops to 0, since none of the four schemes can find a feasible PB transmit power to compensate for the large path loss at long PB-IF distances, and each scheme returns a zero transmit power of the PB.

Fig. 5 shows the PB energy consumption versus P_{\max} under the four different schemes. We can see that when P_{\max} is below 20 dBm, none of the four schemes can find a feasible value of PB transmit power and each sets it to 0. For $P_{\max} > 20$ dBm, the PB energy consumption under the throughput maximization and EE maximization schemes increases with P_{\max} , because they both require the use of maximum possible PB transmit power and transmission time; while under the two proposed schemes, the PB energy consumption decreases with a higher P_{\max} until it reaches 35 dBm. This is because a higher P_{\max} allows each IoT node to use a shorter transmission time τ_k to meet its throughput requirement, and thus a lower circuit energy consumption by each IoT node, which in turn leads to a lower PB transmit power P_0 during the pure EH phase τ_0 in the dynamic PB transmit power scheme or a shorter duration τ_0 of the pure EH phase in the static PB transmit power scheme. When P_{\max} is above 35dBm, the PB energy consumption under the two proposed schemes becomes constant. This is because the optimal value of the PB transmit power under both schemes is well below P_{\max} and the PB

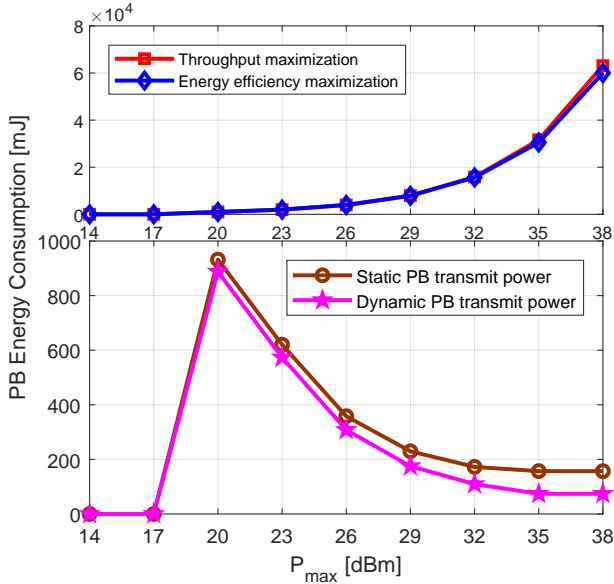


Fig. 5: PB energy consumption versus P_{\max} ($r = 25m$)

energy consumption is thus no longer affected by P_{\max} . Furthermore, the gap between the PB energy consumption of the two proposed schemes becomes larger with P_{\max} before it reaches 35dBm. This is because a higher value of P_{\max} gives the dynamic PB transmit power scheme more flexibility to adjust the PB transmit power in each time slot, thereby further reducing the PB energy consumption as compared with the static PB transmit power scheme.

VII. CONCLUSION

In this paper, we have proposed a dynamic PB transmit power scheme and a reduced complexity static PB transmit power scheme to minimize the PB energy consumption in a wireless powered BackCom network. By analyzing the KKT conditions, we find that the whole time block should be used up for EH and BackCom by all the IoT nodes in order to minimize the PB energy consumption in the dynamic PB transmit power scheme. However, minimizing the energy consumption of the PB in the static PB transmit power scheme does not require the whole time block to be used up. The simulation results show that the proposed algorithms converge very fast and that the dynamic PB transmit power scheme achieves the lowest PB energy consumption compared with the static PB transmit power and the benchmark schemes. The static PB transmit power scheme performs very close to the dynamic scheme but with a reduced implementation complexity. In our future work, we will consider multiple antennas on the PB and the IoT nodes for further improving the system performance.

APPENDIX A

We can see from $\mathcal{P}_{1,2}$ that the objective function (9a) and the constraints (9d) and (9e) are linear. This indicates that the problem $\mathcal{P}_{1,2}$ is convex if and only if the both

constraints (9b) and (9c) are convex. The convexity of constraint (9b) depends on whether $W\tau_k \log_2 \left(1 + \frac{\xi \lambda_k h_k g_k}{\tau_k W N_0}\right) \geq P_k^{\min}$ is a joint concave function with respect to the optimization variables λ_k and τ_k . By using the convexity preserving of the perspective function, we know that the convexity of $W\tau_k \log_2 \left(1 + \frac{\xi \beta_k \theta_k h_k g_k}{\tau_k W N_0}\right)$ is the same as $W \log_2 \left(1 + \frac{\xi \beta_k \theta_k h_k g_k}{W N_0}\right)$, which is a concave function. Thus, the constraint (9b) is convex.

Next we prove that constraint (9c) is convex. For better understanding, we define the following two functions, i.e.,

$$f_1(\theta_k, \lambda_k, \tau_k) = \left(\frac{\frac{a(\theta_k - \lambda_k)}{\tau_k} h_k + d}{\frac{\theta_k - \lambda_k}{\tau_k} h_k + v} - \frac{d}{v} \right) \tau_k, \quad (\text{A.1})$$

$$f_2(\theta_i, \tau_i) = \left(\frac{\frac{a\theta_i}{\tau_i} h_k + d}{\frac{\theta_i}{\tau_i} h_k + v} - \frac{d}{v} \right) \tau_i. \quad (\text{A.2})$$

If both defined functions are joint concave functions with respect with the optimization variables, we can say that the constraint (9c) is concave. As above, it can be derived from the convexity preserving of the perspective function that the convexity of $f_1(\theta_k, \lambda_k, \tau_k)$ and $f_2(\theta_i, \tau_i)$ is determined by $f_3(\theta_k, \lambda_k) = \frac{a(\theta_k - \lambda_k)h_k + d}{(\theta_k - \lambda_k)h_k + v} - \frac{d}{v}$ and $f_4(\theta_i) = \frac{a\theta_i h_k + d}{\theta_i h_k + v} - \frac{d}{v}$, respectively. It can be observed that the convexity of $f_3(\theta_k, \lambda_k)$ and $f_4(\theta_i)$ is highly related with the adopted non-linear EH model $f_5(x) = \frac{ax+d}{x+v} - \frac{d}{v}$, where x is the input power.

As $f_4(\theta_i)$ is simpler than $f_3(\theta_k, \lambda_k)$, in what follows, we first prove that $f_4(\theta_i)$ is a joint concave function and then put our attention on verifying the convexity of $f_3(\theta_k, \lambda_k)$. By comparing $f_4(\theta_i)$ with $f_5(x)$, it is not hard to find that both of them have the same functional form and convexity. The first- and second-order derivatives of $f_5(x)$ can be calculated as, respectively,

$$\frac{\partial f_5}{\partial x} = \frac{av - d}{(x + v)^2}, \quad (\text{A.3})$$

$$\frac{\partial^2 f_5}{\partial x^2} = \frac{2(d - av)}{(x + v)^3}, \quad (\text{A.4})$$

It has been well known that for a practical energy harvester, the output power increases with the input power first and then keeps almost the same when the input power exceed the saturation threshold. Thus, $\frac{\partial f_5}{\partial x} > 0$, which means that $av - d > 0$. Based on this result, we know $\frac{\partial^2 f_5}{\partial x^2} < 0$ if $x + v > 0$. In the practical energy harvester, there exists a saturation threshold, i.e., $\lim_{x \rightarrow \infty} f_5(x) = \frac{av-d}{v} > 0$. Due to $av - d > 0$, we have $v > 0$. Accordingly, $\frac{\partial^2 f_5}{\partial x^2} < 0$ and $f_4(\theta_i)$ is a concave function with respect to θ_i .

The Hessian matrix of $f_3(\theta_k, \lambda_k)$ can be calculated as

$$\nabla^2 f_3(\theta_k, \lambda_k) = \begin{bmatrix} \frac{2(d-av)h_k^2}{[(\theta_k - \lambda_k)h_k + v]^3} & \frac{2(av-d)h_k^2}{[(\theta_k - \lambda_k)h_k + v]^3} \\ \frac{2(av-d)h_k^2}{[(\theta_k - \lambda_k)h_k + v]^3} & \frac{2(d-av)h_k^2}{[(\theta_k - \lambda_k)h_k + v]^3} \end{bmatrix} \quad (\text{A.5})$$

It is not hard to verify that the Hessian matrix in (A.5) is negative semidefinite and thus $f_3(\theta_k, \lambda_k)$ is a joint concave

function.

Based on the above analysis, we confirm that constraint (9c) is convex, and the proof is complete.

APPENDIX B

According to the KKT conditions, $\frac{\partial \mathcal{L}}{\partial \theta_0} = 1 - \sum_{k=1}^K \frac{\alpha_k (av-d)h_k}{\left(\frac{\theta_0}{\tau_0} h_k + v\right)^2} + \omega_0 = 0$ should be satisfied for minimizing the energy consumption of the PB. As proven in Appendix A, $av - d > 0$ holds. Combining $\frac{\partial \mathcal{L}}{\partial \theta_0} = 0$, $av - d > 0$, and $\omega_0 \geq 0$, it is not hard to infer that there is at least one IoT node \hat{k} satisfying $\alpha_{\hat{k}} > 0$. For the \hat{k} -th IoT node, $\frac{\partial \mathcal{L}}{\partial \lambda_{\hat{k}}} = 0$ should be satisfied. Due to $\kappa_{\hat{k}} \geq 0$, we have $\varepsilon_{\hat{k}} > 0$.

Using the complementary slackness conditions $\alpha_{\hat{k}} \left[p_{c,\hat{k}} \tau_{\hat{k}} - \left(\frac{a \left(\frac{\theta_{\hat{k}} - \lambda_{\hat{k}}}{\tau_{\hat{k}}} h_{\hat{k}} + d \right) - \frac{d}{v}}{\frac{\theta_{\hat{k}} - \lambda_{\hat{k}}}{\tau_{\hat{k}}} h_{\hat{k}} + v} \right) \tau_{\hat{k}} - \sum_{i=0, i \neq \hat{k}}^K \left(\frac{a \frac{\theta_i}{\tau_i} h_{\hat{k}} + d}{\frac{\theta_i}{\tau_i} h_{\hat{k}} + v} - \frac{d}{v} \right) \tau_i \right] = 0$ and $\varepsilon_{\hat{k}} \left[R_{\hat{k}}^{\min} - W \tau_{\hat{k}} \log_2 \left(1 + \frac{\xi \lambda_{\hat{k}} h_{\hat{k}} g_{\hat{k}}}{\tau_{\hat{k}} W N_0} \right) \right] = 0$, the equality should be satisfied in both constraints C1'' and C2'' for optimality solving $\mathcal{P}_{1,2}$, which results in Insight 1. The proof is complete.

APPENDIX C

We prove this Insight from the following two steps.

Step 1: As shown in Appendix B, there is at least one IoT node \hat{k} ($\hat{k} \in \{1, 2, \dots, K\}$) satisfying $\alpha_{\hat{k}} > 0$. Since $\frac{\partial \mathcal{L}}{\partial \tau_0} = - \sum_{k=1}^K \alpha_k \left(a - \frac{d}{v} + \frac{(d-av) \left(\frac{2\theta_0}{\tau_0} h_k + v \right)}{\left(\frac{\theta_0}{\tau_0} h_k + v \right)^2} \right) + \vartheta - \omega_0 P_{\max} = 0$, $\vartheta > 0$ holds if the following inequality (C.1) is satisfied.

$$a - \frac{d}{v} + \frac{(d-av) \left(\frac{2\theta_0}{\tau_0} h_k + v \right)}{\left(\frac{\theta_0}{\tau_0} h_k + v \right)^2} > 0. \quad (\text{C.1})$$

To prove (C.1), we construct the following function, i.e.,

$$f_6(h_k) = a - \frac{d}{v} + \frac{(d-av) \left(\frac{2\theta_0}{\tau_0} h_k + v \right)}{\left(\frac{\theta_0}{\tau_0} h_k + v \right)^2}. \quad (\text{C.2})$$

The first-order derivative of $f_6(h_k)$ is calculated as

$$f_6'(h_k) = (av-d) \frac{2 \left(\frac{\theta_0}{\tau_0} \right)^2 h_k}{\left(\frac{\theta_0}{\tau_0} h_k + v \right)^3}. \quad (\text{C.3})$$

Since $av - d > 0$ and $v > 0$, it is not hard to verify that $f_6'(h_k) > 0$ when $h_k \geq 0$. In the practical communication scenario, we have $h_k > 0$, which results in $f_6(h_k) > f_6(0) = 0$, i.e., the inequality (C.1) holds.

Step 2: Combining the complementary slackness condition $\vartheta \left[\sum_{i=0}^K \tau_i - T \right] = 0$ and the result $\vartheta > 0$, we have $\sum_{i=0}^K \tau_i = T$, yielding Insight 2.

The proof is complete.

APPENDIX D

Let us define a function given by $f_1 = \left(\frac{a(1-Y_k)Ph_k+d}{(1-Y_k)Ph_k+v} - \frac{d}{v} \right) \tau_k$, where f_1 is convex with respect to Y_k . Since the first-order Taylor expansion of a convex function is a global under-estimator of its function values. For any given Y_k^j , we have

$$f_1 \geq \left(\frac{a(1-Y_k^j)Ph_k+d}{(1-Y_k^j)Ph_k+v} - \frac{d}{v} \right) \tau_k + \frac{Ph_k d - aPh_k v}{(Ph_k - Y_k^j Ph_k + v)^2} (L_k - Y_k^j \tau_k), \quad (\text{D.1})$$

where the equalities in (D.1) hold when $\frac{L_k}{\tau_k} = Y_k^j$.

The proof is complete.

APPENDIX E

We give the partial Lagrangian function for $\mathcal{P}_{2,1}$, which is a convex problem, as

$$\begin{aligned} \mathcal{L}' = & \sum_{i=0}^K P \tau_i + \sum_{k=1}^K \alpha'_k \left(p_{c,k} \tau_k - E_k^{\text{total}'} \right) + \vartheta' \left(\sum_{i=0}^K \tau_i - T \right) \\ & + \sum_{k=1}^K \varepsilon'_k \left[R_k^{\min} - W \tau_k \log_2 \left(1 + \frac{\xi L_k h_k g_k}{\tau_k W N_0} \right) \right] \\ & + \sum_{k=1}^K \kappa'_k (L_k - \tau_k), \end{aligned} \quad (\text{E.1})$$

where $\alpha'_k, \vartheta', \varepsilon'_k$ and κ'_k are the Lagrange multipliers associated with the constraints in $\mathcal{P}_{2,1}$.

Taking the partial derivative of \mathcal{L}' with respect to $\tau_i, i \in [0, 1, 2, \dots, K]$, there always exists two terms, i.e., $P + \vartheta'$. Since PB transmit power $P > 0, \vartheta' \geq 0$ and based on KKT conditions, ϑ' could be 0 while satisfying $\frac{\partial \mathcal{L}'}{\partial \tau_i} = 0$. Therefore, $\sum_{i=0}^K \tau_i$ could not be equal to T for meeting the complementary slackness condition, that is to say, the available time could not be used up for minimizing the energy consumption of the PB.

The proof is complete.

REFERENCES

- [1] F. Rezaei, C. Tellambura, and S. Herath, "Large-scale wireless-powered networks with backscatter communications— a comprehensive survey," *IEEE Open Journal of the Communications Society*, vol. 1, pp. 1100–1130, 2020.
- [2] M. R. Palattella, M. Dohler, A. Grieco, G. Rizzo, J. Torsner, T. Engel, and L. Ladid, "Internet of things in the 5G era: Enablers, architecture, and business models," *IEEE Journal on Selected Areas in Communications*, vol. 34, no. 3, pp. 510–527, 2016.
- [3] X. Lu, D. Niyato, H. Jiang, D. I. Kim, Y. Xiao, and Z. Han, "Ambient backscatter assisted wireless powered communications," *IEEE Wireless Communications*, vol. 25, no. 2, pp. 170–177, 2018.
- [4] K. Han and K. Huang, "Wirelessly powered backscatter communication networks: Modeling, coverage, and capacity," *IEEE Transactions on Wireless Communications*, vol. 16, no. 4, pp. 2548–2561, 2017.
- [5] B. Lyu, C. You, Z. Yang, and G. Gui, "The optimal control policy for RF-powered backscatter communication networks," *IEEE Transactions on Vehicular Technology*, vol. 67, no. 3, pp. 2804–2808, 2018.

- [6] Y. Xu and G. Gui, "Optimal resource allocation for wireless powered multi-carrier backscatter communication networks," *IEEE Wireless Communications Letters*, vol. 9, no. 8, pp. 1191–1195, 2020.
- [7] B. Clerckx, Z. Bayani Zawawi, and K. Huang, "Wirelessly powered backscatter communications: Waveform design and SNR-energy trade-off," *IEEE Communications Letters*, vol. 21, no. 10, pp. 2234–2237, 2017.
- [8] Z. B. Zawawi, Y. Huang, and B. Clerckx, "Multiuser wirelessly powered backscatter communications: Nonlinearity, waveform design, and SINR-energy tradeoff," *IEEE Transactions on Wireless Communications*, vol. 18, no. 1, pp. 241–253, 2019.
- [9] G. Sacarello and Y. H. Kim, "Rate-energy tradeoffs of wireless powered backscatter communication with power splitting and time switching," *IEEE Access*, vol. 9, pp. 10 844–10 857, 2021.
- [10] Y. Ye, L. Shi, R. Q. Hu, and G. Lu, "Energy-efficient resource allocation for wirelessly powered backscatter communications," *IEEE Communications Letters*, vol. 23, no. 8, pp. 1418–1422, 2019.
- [11] Y. Liu, X. Sheng, K. Fang, L. Shi, and Y. Ye, "Energy efficiency maximization in bistatic backscatter communications with QoS constraint," in *Proceedings of IEEE 19th International Conference on Communication Technology (ICCT)*, 2019, pp. 920–925.
- [12] H. Yang, Y. Ye, and X. Chu, "Max-min energy-efficient resource allocation for wireless powered backscatter networks," *IEEE Wireless Communications Letters*, vol. 9, no. 5, pp. 688–692, 2020.
- [13] D. Li and Y. Liang, "Price-based bandwidth allocation for backscatter communication with bandwidth constraints," *IEEE Transactions on Wireless Communications*, vol. 18, no. 11, pp. 5170–5180, 2019.
- [14] N. Van Huynh, D. T. Hoang, D. Niyato, P. Wang, and D. I. Kim, "Optimal time scheduling for wireless-powered backscatter communication networks," *IEEE Wireless Communications Letters*, vol. 7, no. 5, pp. 820–823, 2018.
- [15] S. H. Kim and D. I. Kim, "Hybrid backscatter communication for wireless-powered heterogeneous networks," *IEEE Transactions on Wireless Communications*, vol. 16, no. 10, pp. 6557–6570, 2017.
- [16] B. Lyu, H. Guo, Z. Yang, and G. Gui, "Throughput maximization for hybrid backscatter assisted cognitive wireless powered radio networks," *IEEE Internet of Things Journal*, vol. 5, no. 3, pp. 2015–2024, 2018.
- [17] Y. Ye, L. Shi, X. Chu, and G. Lu, "Throughput fairness guarantee in wireless powered backscatter communications with HTT," *IEEE Wireless Communications Letters*, pp. 1–1, 2020.
- [18] B. Lyu, D. T. Hoang, and Z. Yang, "Backscatter then forward: A relaying scheme for batteryless IoT networks," *IEEE Wireless Communications Letters*, vol. 9, no. 4, pp. 562–566, 2020.
- [19] D. Li, "Two birds with one stone: Exploiting decode-and-forward relaying for opportunistic ambient backscattering," *IEEE Transactions on Communications*, vol. 68, no. 3, pp. 1405–1416, 2020.
- [20] R. Kishore, S. Gurugopinath, P. C. Sofotasios, S. Muhaidat, and N. Al-Dhahir, "Opportunistic ambient backscatter communication in RF-powered cognitive radio networks," *IEEE Transactions on Cognitive Communications and Networking*, vol. 5, no. 2, pp. 413–426, 2019.
- [21] L. Shi, R. Q. Hu, J. Gunther, Y. Ye, and H. Zhang, "Energy efficiency for RF-powered backscatter networks using HTT protocol," *IEEE Transactions on Vehicular Technology*, vol. 69, no. 11, pp. 13 932–13 936, 2020.
- [22] S. Ma, G. Wang, R. Fan, and C. Tellambura, "Blind channel estimation for ambient backscatter communication systems," *IEEE Communications Letters*, vol. 22, no. 6, pp. 1296–1299, 2018.
- [23] W. Zhao, G. Wang, S. Atapattu, R. He, and Y.-C. Liang, "Channel estimation for ambient backscatter communication systems with massive-antenna reader," *IEEE Transactions on Vehicular Technology*, vol. 68, no. 8, pp. 8254–8258, 2019.
- [24] D. Mishra and E. G. Larsson, "Optimal channel estimation for reciprocity-based backscattering with a full-duplex MIMO reader," *IEEE Transactions on Signal Processing*, vol. 67, no. 6, pp. 1662–1677, 2019.
- [25] Y. Chen, N. Zhao, and M. Alouini, "Wireless energy harvesting using signals from multiple fading channels," *IEEE Transactions on Communications*, vol. 65, no. 11, pp. 5027–5039, 2017.
- [26] S. Boyd, *Convex optimization*. Cambridge, UK: Cambridge University Press, 2004.
- [27] M. Hua, L. Yang, C. Li, Q. Wu, and A. L. Swindlehurst, "Throughput maximization for UAV-aided backscatter communication networks," *IEEE Transactions on Communications*, vol. 68, no. 2, pp. 1254–1270, 2020.
- [28] H. Yang, Y. Ye, X. Chu, and S. Sun, "Energy efficiency maximization for uav-enabled hybrid backscatter-harvest-then-transmit communications," *IEEE Transactions on Wireless Communications*, pp. 1–1, 2021.
- [29] Y. Ye, L. Shi, X. Chu, D. Li, and G. Lu, "Delay minimization in wireless powered mobile edge computing with hybrid backcom and AT," *IEEE Wireless Communications Letters*, vol. 10, no. 7, pp. 1532–1536, 2021.